The Structure of White Dwarf Stars Using Computational Methods

N. Khan[a)]

(Dated: 20 November 2017)

Using a model based on the internal force balance of a white dwarf, and solved using the Runge-Kutta method, the central densities of three observed white dwarfs, Sirius B, 40 Eri B and Stein 2051 were calculated to be $(4.5 \pm 1.17) \times 10^{10} kgm^{-3}$, $(2.59 \pm 0.59) \times 10^{9} kgm^{-3}$ and $(3.86 \pm 3.77) \times 10^{9} kgm^{-3}$. Sirius B is suspected to be a white dwarf of carbon composition while 40 Eri B and Stein 2051 are likely to be composed of iron. An estimate of the Chandrasekhar limit was found to be $\approx 1.44 M_{\odot}$, which is in agreement with pre-existing literature, and an upper mass limit for a theoretical white dwarf composed of 100% iron-56 was found to be $\approx 1.24 M_{\odot}$.

Keywords: White Dwarf, Runge Kutta, Hydrostatic Equilibrium, Chandrasekhar Limit, Central Density

I. INTRODUCTION

A white dwarf is the end product of stars with initial masses from about 0.07 to 8 $M_{\odot}$ which comprises around 97% of the stars in our galaxy.[1] It therefore represents the most common evolutionary endpoint of most stars including our sun. Of cosmological importance, the long timescales involved in a fusion-less white dwarf provide a map of the past evolutionary track for the star and the surrounding environment,[2] potentially providing valuable information on stellar and galactic evolution.[3]

Composed mostly of electron-degenerate matter, white dwarfs resist collapsing into denser stellar objects such as neutron stars or black holes by the balance of electron degeneracy pressure and gravity,[4,5] this balance is key in the determination of white dwarf properties such as mass, radius, central density and elemental composition of the star. Such calculations are often analytically challenging and so computational numerical methods provide a robust and efficient tool to tackle such problems.

II. BACKGROUND PHYSICS

A. Hydrostatic equilibrium and force balance

A star may be modelled as a spherically symmetric, non rotating mass of gas. The force balance between the gravitational force attempting to collapse the star and the gas pressure opposing it can be described using the equation of hydrostatic equilibrium.

$$\frac{dP}{dr} = -\frac{Gm(r)}{r^2}\rho(r) \tag{1}$$

Which relates the Pressure P, radius r, mass $m(r)$, and density $\rho(r)$. Which, by using the chain rule, may be rewritten as

$$\frac{dP}{dr} = \frac{d\rho}{dr}\frac{dP}{d\rho} \tag{2}$$

The $\frac{dP}{d\rho}$ term in eq (2) is only dependent on the materials of which the star is composed, and thus constitutes an equation of state. In most main sequence stars the gas pressure may be modelled as thermal pressure using the ideal gas law, however for objects subject to greater forces like white dwarfs, the composing matter will behave as degenerate fermions, and so a reasonable approximation to this equation of state can be modelled using the relativistic free Fermi gas.[6]

$$\frac{dP}{d\rho} = Y_e \frac{m_e c^2}{m_p} \gamma \left(\frac{\rho(r)}{\rho_0}\right) \tag{3}$$

ρ_0 is in units of $kg\ m^{-3}$ and provides natural unit for density given by

$$\rho_0 = \frac{m_p m_e^3 c^3}{3\pi^2 \hbar^3 Y_e} = \frac{9.79 \times 10^8}{Y_e} \tag{4}$$

where Y_e is the number of electrons per nucleon, c the speed of light, m_e and m_p the electron and proton masses.

The γ function is given by

$$\gamma(y) = \frac{y^{2/3}}{3(1+y^{2/3})^{1/2}} \tag{5}$$

combining equations (1) and (3) we reach a differential equation given by

$$\frac{d\rho}{dr} = -\left(\frac{dP}{d\rho}\right)^{-1} \frac{Gm(r)}{r^2}\rho(r) \tag{6}$$

Using connected rates of change of the above equation with the relationship between the the mass and radius of a thin spherical shell (7), we can use what is known as the Runge-Kutta method to solve numerically for the density and mass and radius of the star.

$$\frac{dm}{dr} = 4\pi r^2 \rho(r) \tag{7}$$

III. COMPUTATIONAL DETAILS

A. Nondimensionalisation of mass and density functions

Due to the large quantities involved in astronomical systems, if equations (6) and (7) are to be solved nu-

[a)]School of Physics and Astronomy, University of Southampton; Electronic mail: nk7g14@soton.ac.uk

merically they must first be scaled appropriately. The variables present in the equations are r, $\rho(r)$ and $m(r)$ and so we aim to recast these in a manner that is dimensionless. Therefore each variable must scaled using a constant (characteristic unit) that is of the same dimensions. We will denote the new dimensionless variable with a dash and the characteristic unit with a nought.

$$\begin{aligned} \rho(r) \to \rho'(r) &= \frac{\rho(r)}{\rho_0} \\ m(r) \to m'(r) &= \frac{m(r)}{M_0} \\ r \to r' &= \frac{r}{R_0} \end{aligned} \tag{8}$$

For the density constant, ρ_0 we equate it to the definition from equation (4). The choice of the constant may be any combination of variables or number that is dimensionally correct, however it is sensible to use units that are characteristic to the system in question. Similarly we may also chose characteristic units for M_0 and R_0 that are given by

$$M_0 = \frac{4}{3}\pi\rho_0 R_0^3 \tag{9}$$

$$R_0 = \left(\frac{3Y_e m_e c^2}{4\pi G m_p \rho_0}\right)^{1/2} \tag{10}$$

replacing the variables in equations (6) and (7) with those from (8) using the steps found in appendices VII A and VII B we obtain two new dimensionless relations:

$$\frac{d\rho'}{dr'} = -\frac{m'(r')\rho'(r')}{r'^2} \tag{11}$$

and

$$\frac{dm'}{dr'} = 3r'^2\rho'(r') \tag{12}$$

B. Runge-Kutta algorithm

Equations (11) and (12) can be numerically integrated via the use of the the fourth order Runge-Kutta method, the literature on which is quite expansive[7] and so most details will be spared in this paper. The key points to note however is that the iterative integration process takes place via a step size of h and is run n times.

Since we have nondimensionalised the equations we are solving so that they are unitary, the step size can be set to $h = 1/n$ meaning that we can continually change the number of iterations until we reach a desirable accuracy, this type of approach is what is known as an adaptive Runge-Kutta Method. An important note is that more iterations will increase computational time and yet does not imply higher accuracy[8] as reducing h will result in more steps to reach the same endpoint, therefore it may be useful to use a small step size where the solution is rapidly changing and vice versa, however this will lead to the unequal tabulation of data, and so at cost of accuracy, a constant small step was chosen for the specific integration in question.

1. Calculation of uncertainty

The Runge-Kutta algorithm iterates from a value x_1 to the next value x_2, giving a value of y_1 with an associated uncertainty δ. The value of δ may be quantised by reducing the step size h by a factor, say $1/2$, giving a new, slightly changed, value of y_1 we denote by y_1' thus we can calculate

$$\delta = \frac{y_1' - y_1}{y_1} \tag{13}$$

Thus by changing the step size we can control the uncertainty to a point that is desirable, for our case we chose this uncertainty to be $< 0.0001\%$ Thus all values for density, mass and radius are quoted to below this mathematical uncertainty unless otherwise stated.

IV. RESULTS AND DISCUSSIONS

A. Internal structure of white dwarf stars

Using the methods in III we solved for the internal structure of theoretical white dwarfs. The first calculation was for the comparison two white dwarfs composed of 100% carbon-12($Y_e = 0.5$) and iron-56 ($Y_e = 26/56$) = 0.464.

The star was integrated with initial boundary conditions of $r = 0$, and central density $\rho(0) = \rho_0$, to final boundary condition of $\rho(r) = 0$. Plotting the two stars with mass against radius we obtained FIG. 1.

TABLE I. Tabulated results for carbon and iron based white dwarfs with two different central densities.

Type	**Central Density**	**Mass ($M_\odot$)**	**Radius ($R_\odot$)**
Carbon	ρ_0	0.504	0.0139
Iron	ρ_0	0.434	0.0129
Carbon	$10^5\rho_0$	1.422	0.00155
Iron	$10^5\rho_0$	1.226	0.00144

From FIG. 1. it can be seen that the carbon white dwarf reaches a larger mass and radius than an iron star of equal central density.

Performing the same calculation, taking the upper limit of the central density by setting it to $10^5\rho_0$, we obtain FIG. 2, we observe the mass for the carbon white dwarf to be asymptotic to around $\approx 1.42 M_\odot$ and the iron

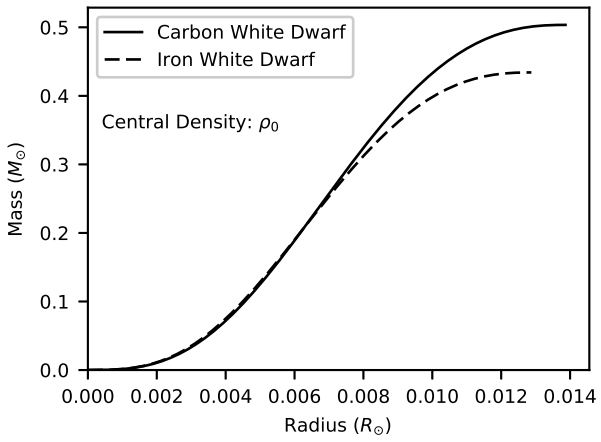

FIG. 1. Comparison of carbon and iron based white dwarfs internal mass radius relationship with central density ρ_0.

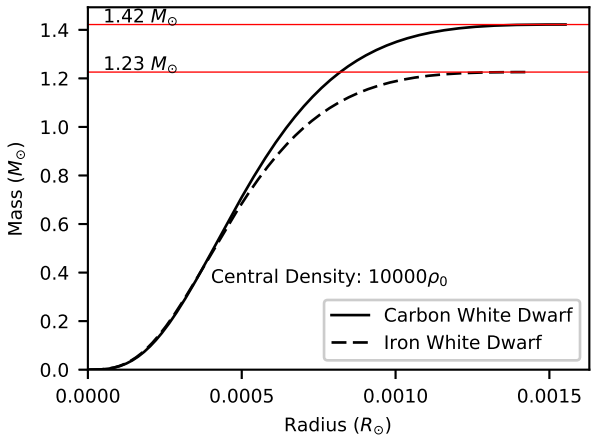

FIG. 2. Comparison of carbon and iron based white dwarfs internal mass radius relationship with central density $10^5\rho_0$.

star to $\approx 1.23M_\odot$. Increasing the density to higher values further reduces the radius however this upper limit of the mass does not increase significantly, as seen in FIG. 3.

This upper limit for the mass of white white dwarf is what is known as the Chandrasekhar limit, of which the currently accepted value is around $\approx 1.44M_\odot$,[9] although this may not be set in stone as a paper published in 2013 by Das and Mukhopadhyay[10] suggest an upper limit of $\approx 2.58M_\odot$ based on observed super-luminous white dwarfs. The accepted result however is a result of the relativistic nature of the free Fermi gas present in white dwarfs. If a white dwarf were to exceed this mass, by having it's central density go to infinity, the matter would no longer behave as fermions and would likely collapse into other extreme stellar objects such as neutron stars or black holes. It is interesting to note that a iron white dwarf seems to have an upper limit of $\approx 1.24M_\odot$, this is an unusual observation as stars that would be of this nature would likely undergo a core collapse supernova[11]

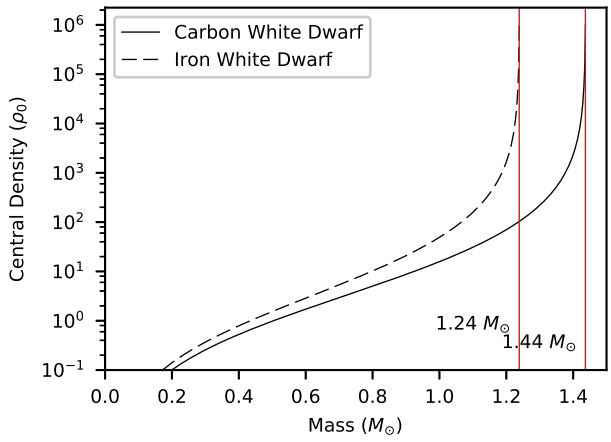

FIG. 3. Graph showing central density agaist mass, the two maximum masses for the carbon and iron dwarfs are labelled.

We may also plot the internal density relation for the two stars in the same way as we have done with their mass, these plots are found and discussed in appendices VII C.

B. Mass-radius dependence on central density

Plots were made to analyse the effects of central density on mass and radius. This was done by simulating N number of stars with different central densities and plotting their mass against radius. On the graph was also plotted the mass and radius of three known white dwarfs[12] shown in table II.

TABLE II. Mass, radius, and calculated theoretical central density (TCD) of three known white dwarfs.

Name	**Mass** ($M_\odot$)	**Radius** ($R_\odot$)	**TCD** (ρ_0)
Sirius B	1.053 ± 0.028	0.0074 ± 0.0006	23.0 ± 6.0
40 Eri B	0.48 ± 0.02	0.0124 ± 0.0005	1.23 ± 0.28
Stein 2051	0.50 ± 0.05	0.0115 ± 0.0012	1.83 ± 1.79

400 stars of carbon and iron were simulated with central densities spread in a logarithmic fashion between $(0.01\rho_0$ to $10^6)\rho_0$, these are shown on FIG. 4 of which a zoomed plot is shown on FIG. 5, also shown are the 3 known stars from table II with associated error bars. We note that Sirius A coincides with a carbon white dwarf with central density $\approx (23.0 \pm 6.0)\rho_0$. 40 Eri B and Stein 2051 correspond to iron based white dwarfs with central densities of $\approx (1.23 \pm 0.28)\rho_0$ and $\approx (1.83 \pm 1.79)\rho_0$ respectively. Which, in SI units, gives $(4.5 \pm 1.17) \times 10^{10} kgm^{-3}$, $(2.59 \pm 0.59) \times 10^9 kgm^{-3}$ and $(3.86 \pm 3.77) \times 10^9 kgm^{-3}$. The errors of these values were calculated by taking the upper and lower limits of radius and thus corresponding

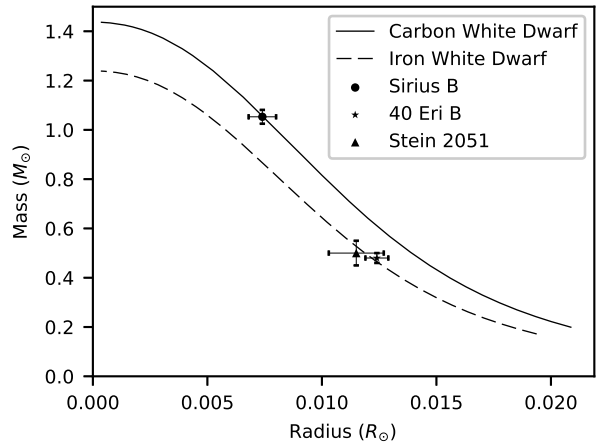

FIG. 4. Mass-radius relation for 400 stars with central densities between $0.1\rho_0$ and $10^6\rho_0$.

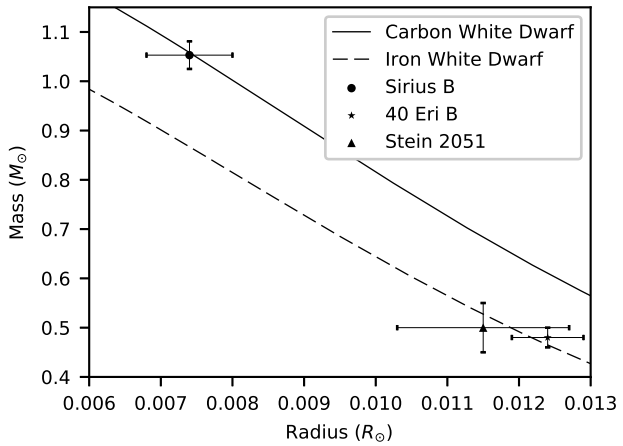

FIG. 5. Zoomed version of FIG. 4.

upper and lower limit of central density.

V. CONCLUSION

Using a model of the force balance between the relativistic free Fermi gas and the equation of hydrostatic equilibrium, we have obtained estimates for the central density and compositions of two iron based white dwarfs, 40 Eri B and Stein 2051 with central densities $\approx (1.23 \pm 0.28)\rho_0$ and $\approx (1.83 \pm 1.79)\rho_0$ and for the carbon based white dwarf Sirius B with central density $\approx (23.0 \pm 6.0)\rho_0$. We have also determined the Chandrasekhar limit for an iron white dwarf to be $\approx 1.44M_\odot$ and that for a theoretical upper limit to a iron based white dwarf of $\approx 1.24M_\odot$. Possible extensions involve using models that do not have singular elemental compositions, which may allow for some deviations from the theoretical curve that may explain the slight deviations that 40 Eri B and Stein 2051 display. The model we have used also does not have any temperature dependence which could play a roll in the calculation of degeneracy pressure. Mathematically, the solving of the Lane Emden equation of state may also provide another method to probe the internal structure of white dwarfs.[13]

VI. REFERENCES

[1] G. Fontaine, P. Brassard, and P. Bergeron, "The Potential of White Dwarf Cosmochronology," Publications of the ASP **113**, 409–435 (2001).

[2] J. B. Holberg, "How Degenerate Stars Came to be Known as White Dwarfs," in *American Astronomical Society Meeting Abstracts*, Bulletin of the American Astronomical Society, Vol. 37 (2005) p. 1503.

[3] R. Stothers, "White dwarfs, the Galaxy and Dirac's cosmology," Nature **262**, 477–479 (1976).

[4] R. Canal and J. Gutierrez, "The possible white dwarf-neutron star connection," Astrophys. Space Sci. Libr. **214**, 49 (1997), arXiv:astro-ph/9701225 [astro-ph].

[5] S. Chandrasekhar and S. Chandrasekhar, *An introduction to the study of stellar structure*, Vol. 2 (Courier Corporation, 1958).

[6] I. Sagert, M. Hempel, C. Greiner, and J. Schaffner-Bielich, "Compact stars for undergraduates," Eur. J. Phys. **27**, 577–610 (2006), arXiv:astro-ph/0506417 [astro-ph].

[7] J. C. Butcher, "A history of runge-kutta methods," Appl. Numer. Math. **20**, 247–260 (1996).

[8] W. H. Press and W. H. Press, "6.2 adaptive stepsize control for runge-kutta," in *Numerical recipes in C: the art of scientific computing* (Cambridge University Press, 1986) pp. 714–722.

[9] S. Chandrasekhar, "The highly collapsed configurations of a stellar mass (Second paper)," Mon. Not. R. Astron. Soc. **95**, 207–225 (1935).

[10] U. Das and B. Mukhopadhyay, "New mass limit for white dwarfs: Super-chandrasekhar type ia supernova as a new standard candle," Phys. Rev. Lett. **110**, 071102 (2013).

[11] *Astrophysik II: Sternaufbau/Astrophysics II: Stellar Structure* (Springer Berlin, 2013).

[12] J. L. Provencal, H. L. Shipman, E. Hg, and P. Thejll, "Testing the white dwarf mass-radius relation with hipparcos," The Astrophysical Journal **494**, 759 (1998).

[13] A.-M. Wazwaz, "A new algorithm for solving differential equations of laneemden type," Applied Mathematics and Computation **118**, 287 – 310 (2001).

VII. APPENDICES

A. Derivation for density-radius nondimensionalisation

Expanding eq. 6 we have

$$\frac{d\rho}{dr} = -\frac{Gm_p}{Y_e m_e c^2}\frac{1}{\gamma\left(\rho(r)/\rho_0\right)}\frac{m(r)\rho(r)}{r^2} \tag{14}$$

Replacing

$$\begin{aligned} m(r) &= M_0 m'(r') \\ \rho(r) &= \rho_0 \rho'(r') \\ r &= R_0 r' \end{aligned} \tag{15}$$

Where

$$M_0 = \frac{4}{3}\pi\rho_0 R_0^3 \tag{16}$$

$$\rho_0 = \frac{m_p m_e^3 c^3}{3\pi^2\hbar^3 Y_e} \tag{17}$$

and by using the relation

$$\frac{d\rho}{dr} = \frac{dr'}{dr}\frac{d\rho}{dr'} = \frac{dr'}{dr}\left(\frac{d\rho}{d\rho'}\frac{d\rho'}{dr'}\right) = \frac{1}{R_0}\left(\rho_0\frac{d\rho'}{dr'}\right) \tag{18}$$

We obtain

$$\frac{\rho_0}{R_0}\frac{d\rho'}{dr'} = -\frac{Gm_p}{Y_e m_e c^2}\frac{1}{\gamma\left(\rho'(r')\right)}\frac{M_0 m'(r')\rho_0\rho'(r')}{(R_0 r')^2} \tag{19}$$

Simplifying

$$\frac{d\rho'}{dr'} = -\frac{Gm_p M_0}{Y_e m_e c^2 R_0}\frac{m'(r')\rho'(r')}{\gamma\left(\rho'(r')\right)r'^2} \tag{20}$$

By substituting the definition of M_0 in, we find

$$\frac{d\rho'}{dr'} = -\frac{Gm_p}{Y_e m_e c^2}\frac{4\pi R_0^2\rho_0}{3}\frac{m'(r')\rho'(r')}{\gamma\left(\rho'(r')\right)r'^2} \tag{21}$$

We wish to normalize the above equation so that all the constants not dependent on r are unitary.

$$\begin{aligned} \frac{Gm_p}{Y_e m_e c^2}\frac{4\pi R_0^2\rho_0}{3} &= 1 \\ \therefore R_0 &= \left(\frac{3Y_e m_e c^2}{4\pi G m_p \rho_0}\right)^{1/2} \end{aligned} \tag{22}$$

The dimensions of R_0 are in meters.

$$\left[\frac{[kg][m^2\cdot s^{-2}]}{[m^3\cdot kg^{-1}\cdot s^{-2}][kg][kg\cdot m^{-3}]}\right]^{1/2} = [m^2]^{1/2} = [m] \tag{23}$$

Thus, our final nondimensionalised equation for the density radius relation is

$$\frac{d\rho'}{dr'} = -\frac{m'(r')\rho'(r')}{r'^2} \tag{24}$$

B. Derivation for mass-radius nondimensionalisation

Starting with

$$\frac{dm}{dr} = 4\pi r^2\rho(r) \tag{25}$$

Replacing

$$\begin{aligned} m(r) &= M_0 m'(r') \\ \rho(r) &= \rho_0\rho'(r') \\ r &= R_0 r' \end{aligned} \tag{26}$$

and by using the relation

$$\frac{dm}{dr} = \frac{dr'}{dr}\frac{dm}{dr'} = \frac{dr'}{dr}\left(\frac{dm}{dm'}\frac{dm'}{dr'}\right) = \frac{1}{R_0}\left(M_0\frac{dm'}{dr'}\right) \tag{27}$$

we obtain

$$\frac{M_0}{R_0}\frac{dm'}{dr'} = 4\pi(R_0 r')^2\rho_0\rho'(r') \tag{28}$$

Simplifying

$$\frac{dm'}{dr'} = \frac{4\pi R_0^3\rho_0}{M_0}r'^2\rho'(r') \tag{29}$$

Inserting the value of $M_0 = 4\pi R_0^3\rho_0/3$ in the above equation we obtain the final nondimensionalised relation

$$\frac{dm'}{dr'} = 3r'^2\rho'(r') \tag{30}$$

C. Density-radius plots for internal structure

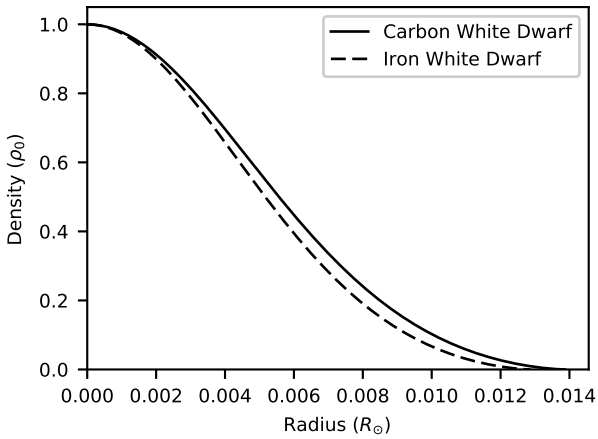

FIG. 6. Comparison of carbon and iron based white dwarfs internal density radius relationship with central density ρ_0

We see from figures 6 and 7 that the average density for the iron white dwarf is less than that of the carbon star, and a higher central density results in steeper density fall off.

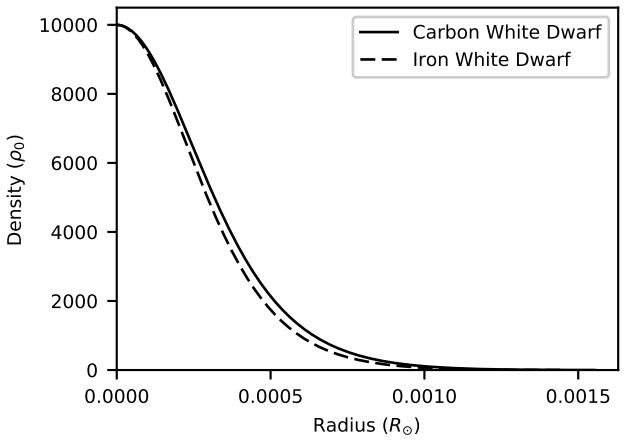

FIG. 7. Comparison of carbon and iron based white dwarfs internal density radius relationship with central density $10000\rho_0$